STUDY ON THE PARAMETERIZATION OF TRAPEZOIDAL MODEL FOR SURFACE MOISTURE ESTIMATION

Hugo Tameirão Seixas, Marcelo Cardoso da Silva Bandoria, Matheus Costa Coldibeli, Elisabete Caria Moraes, Ieda Del'Arco Sanches

National Institute of Spatial Research – INPE, Mailbox 515 - 12227-010 - São José dos Campos - SP, Brasil
{hugo.seixas, marcelo.bandoria, matheus.coldibeli, ieda.sanches}@inpe.br, bete@dsr.inpe.br

ABSTRACT

Soil moisture can be estimated by three approaches using remote sensing techniques, optical, thermal, and microwave methods. The use of optical methods has the advantage of relying only on data from optical sensors, which have high availability, high spatial and temporal resolution, and don't rely on field collected data. For example, the OPTRAM (Optical Trapezoid Model) is based on a linear relationship between soil moisture and a transformed short-wave infrared (STR) reflectance, and hypothetically requires only one parameterization for a region, and can be reproduced on different dates, being invariant to the time of data acquisition [1]. In this context, the objective of the present work is to evaluate different methods for the parameterization of the trapezoidal model to estimate soil moisture.

Keywords — Orbital remote sensing; Soil moisture; Sentinel-2; OPTRAM.

1. INTRODUCTION

The determination of soil moisture is a challenge for several areas of knowledge, from those applied to precision agriculture, to other studies that seek to associate such parameters with other variables of the soil interface and atmosphere, in order to understand the distribution of moisture on the surface.

Soil moisture can be estimated through three approaches using remote sensing techniques, optical, thermal, and microwave methods. The use of microwave sensors on board satellites already presents robust methodologies for estimation of soil surface moisture at global scales, however the scale reduction is necessary for its application in hydrological processes and agriculture [2]. The hypothesis is that this limitation can be overcome through the use of optical methods, which has the advantage of being dependent only on data from optical sensors that are numerous and provide a big amount of data in high spatial and temporal resolution [1].

One of the available methods for estimating soil moisture from optical remote sensing is the OPTRAM, proposed by [1], which is based on a linear relationship between soil moisture and transformed short-wave infrared reflectance (STR) [3], and hypothetically requires only one parameterization for a given region. In order to obtain soil moisture values from the OPTRAM, a pixel distribution with the normalized difference vegetation index (NDVI) and STR

values is used. It is expected that the distribution of pixels will form a trapezoidal shape, due to the linear relation between water content in soils and vegetation.

As a recent model, it is necessary to carry out further studies on the behaviour of OPTRAM in different regions [1], using different methods in their parameterization to evaluate which would be the most indicated in each situation. Considering this need, the present work has the objective of evaluating different parameters in the calibration of the OPTRAM model to estimate soil moisture in a centre pivot irrigated agricultural area, cultivated with annual crops. The parameters analysed will be the number of scenes used, the size of the pixels, and the use of masks in the scenes to remove non-agricultural areas.

2. MATERIAL AND METHODS

The study was carried out in an intensive agricultural area located in Campo Novo do Parecis, state of Mato Grosso, in the Center-West Region of Brazil. It is located at the coordinates 13º40'31"S, 57º53'31"W.

A total of 9 Sentinel-2, level 1C images, between the dates of July 19, 2017 and July 14, 2018 were used. The total extent of the scenes were used in the parameterization of the model, while for the elaboration of the humidity map, it was used only a fragment of the image of May 25, 2018.

After obtaining the images, the atmospheric correction was performed through the Sen2Cor [4] application in conjunction with the SNAP software. To make the bands of the images compatible with each other, the resampling of the bands with spatial resolution of 20 and 60 meters for a pixel size of 10 meters were made, since it is the smallest resolution available in four bands of an image of the Sentinel 2 satellites. After that, operations were performed between bands to obtain the STR and NDVI indices, according to Equations 1 and 2, respectively:

$$STR = \frac{(1-R_{SWIR})^2}{2*R_{SWIR}} \qquad \text{Equation 1}$$

$$NDVI = \frac{(NIR-Red)}{(NIR+Red)} \qquad \text{Equation 2}$$

For the parameterization of the OPTRAM, 5 scenarios were created as described below:

• Use of 9 images using a pixel size of 120m. It was considered as the reference map [1];
• Use of 9 images with pixel size of 60m;
• Use of 9 images with pixel size of 10m;
• Use of 4 images with pixel size of 120m;

• Use of 9 images, without the removal of non-agricultural areas, with pixels size of 120m.

The processes performed in this work, from obtaining the images to the creation of the soil moisture maps are shown in Figure 1.
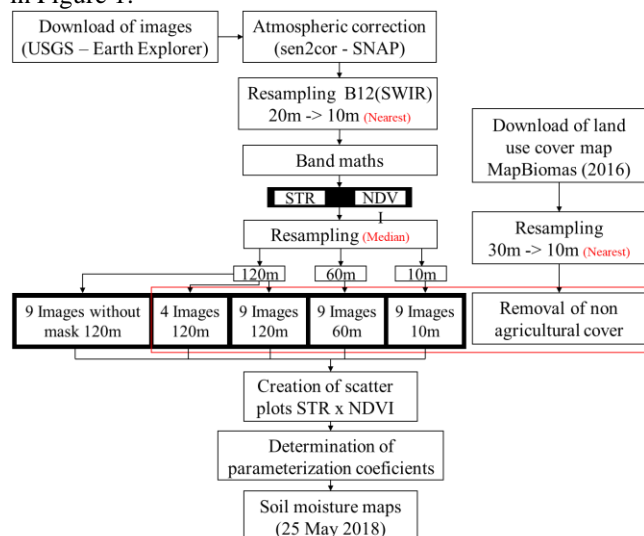

Figure 1. Flow chart of the carried out processes in this study.

To obtain images with larger pixel sizes than 10 meters, resampling were made by adopting the method of medians, which gives the new resampled pixel the median value of all pixels inside its area.

The separation of the agricultural areas from the others was done through based on the MapBiomas land use classification map for the year 2016. Even with the discrepancy between the years of MapBiomas map and the images analyzed in the present study, a visual assessment indicated that the use of these data was adequate to obtain the mask of agricultural areas.

After treating the images for each scenario, scatter graphs of pixel dispersion of the STR and NDVI images were generated. From the visual interpretation of each dispersion graph, the necessary coefficients were obtained for the parameterization of the model. Figure 2 illustrates the interpretation of the dispersion of pixels in the graph.
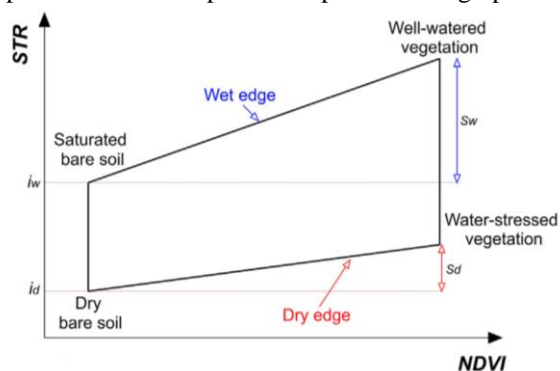

Figure 2. Theoretical dispersion of STR and NDVI pixels to the acquisition of the parameterization coefficients, *iw* (wet edge intercept), *sw* (wet edge slope), *id* (dry edge intercept), and *sd* (dry edge slope). Taken from [5].

After obtaining the coefficients, Equation 3 was applied to obtain the normalized soil moisture index.

$$W = \frac{i_d + s_d * NDVI - STR}{i_d - i_w + (s_d - s_w) * NDVI}$$ *Equation 3*

The data were analyzed through the descriptive statistics of the normalized soil moisture (W) maps and the Wilcoxon test, comparing a stratified random sample of 120 points in the maps obtained, in order to evaluate if there were significant differences between the alternative scenarios and the reference scenario.

3. RESULTS

The scatter graphs generated for each scenario presented, in most cases, a higher concentration of points in the region of STR values between 0 and 6. Only the scenario of *9 Images 10m* presented higher occurrence of pixels with higher STR values in the NDVI region of less than 0.8 (Figure 3).
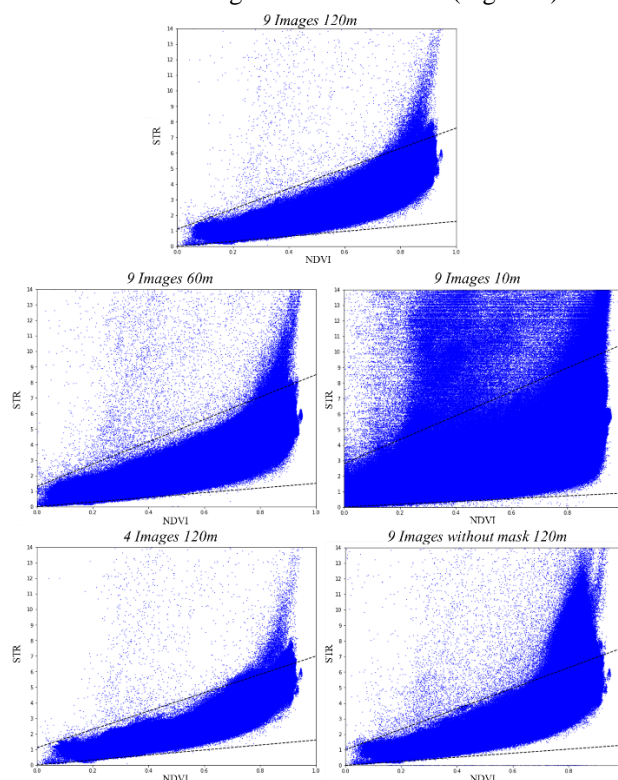

Figure 3. Scatter graphs of each scenario. The horizontal axes represents the NDVI, and the vertical axis the STR.

From the visual interpretation of each dispersion graph, the parameterization coefficients (*iw*, *id*, *sd* and *sw*), used to calculate the normalized moisture estimate (W), were obtained (Table 1).

Table 1. Parametrization coefficients for each scenario.

	9 Images 120m	9 Images 60m	9 Images 10m	4 Images 120m	9 Images without Mask 120m
id	0.0	0.0	0.0	0.0	0.0
sd	0.9	1.5	1.6	1.6	1.3
iw	2.8	1.3	1.1	1.2	1.0
sw	7.7	7.2	6.5	5.8	6.6

With the parameterization coefficients, it was possible to produce the normalized soil moisture (W) maps from Equation 3 for each scenario (Figure 4). The values of soil moisture vary between 0 and 1, being dimensionless due to its normalization.
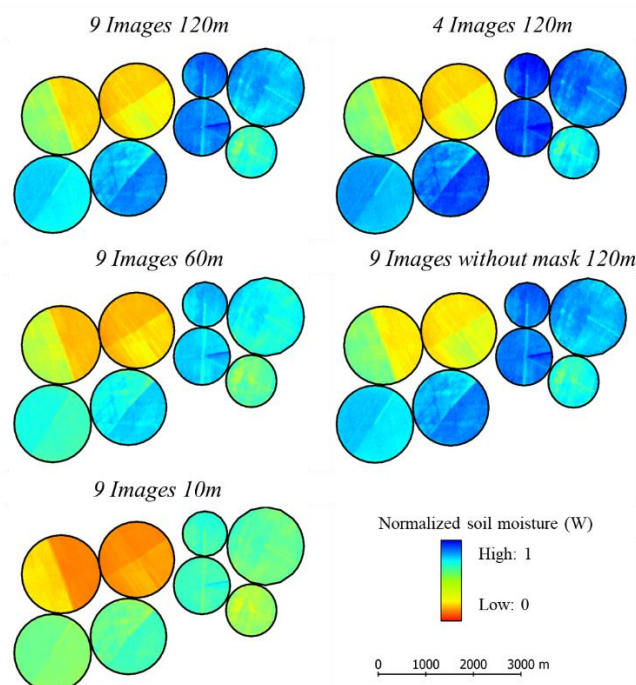

Figure 4. Normalized soil moisture (W) maps for all scenarios.

From each generated map, the descriptive statistics were obtained, in order to perform an exploration of the characteristics of the results (Table 2). It is possible to observe some differences of average values between the scenarios, being that *9 Images 10m* was the one that presented the lowest mean. There is also a greater variation in the maximum values of soil moisture in relation to the minimum values. Changes in the variance in the scenarios indicate that the dispersion of the results also presented differences.

Table 2. Descriptive statistics of normalized soil moisture (W) of each scenario.

Image	Min	Max	Average	Std. Deviation	Variance
NDVI	0.132	0.945	0.699	0.303	0.091
STR	0.795	7.254	4.151	2.043	4.174
W (*9 Images 120m*)	0.123	1.053	0.609	0.201	0.040
W (*9 Images 60m*)	0.120	0.916	0.533	0.174	0.030
W (*9 images10m*)	0.147	0.720	0.426	0.152	0.023
W (*4 Images 120m*)	0.136	1.165	0.666	0.232	0.053
W (*9 Images without Mask 120m*)	0.164	1.052	0.628	0.192	0.036

A non-parametric Wilcoxon paired test was used to obtain statistical evidence that there were significant differences between the maps obtained from each scenario (Table 3). The null hypothesis of the test is that there is no evidence that the samples show any significant difference. The test was performed by comparing the reference scenario (*9 Images 120m*) with the others.

Table 3. Wilcoxon test for normalized soil moisture (W) of the proposed scenarios, considering a confidence level of 95%.

Wilcoxon test	*9 Images 60m*	*9 Images 10m*	*4 Images 120m*	*9 Images without Mask 120m*
	P-value	P-value	P-value	P-value
9 Images 120m	8.963e-05*	4.738e-13*	0.003868*	0.2493

The Wilcoxon test shows that only the scenario *9 Images without Mask 120m* did not show significant differences with the reference scenario. Tests from all other scenarios pointed sufficient evidence to reject the hypothesis that there were no significant differences in relation to the baseline scenario.

4. DISCUSSION

The observed changes in the distribution of the pixels in the dispersion graphs have an effect on the parameterization of the model, and consequently, alter the final soil moisture (W) results. Because it is a visual method of parametrization, the perception of the trapezoid can be subjective, and ends up introducing errors in the final result. On the other hand, the parameterization by visual interpretation is not strongly affected by extreme data, which could have a significant effect in the case of automatic methodologies for the determination of the parameterization coefficients.

Observing the scatter plots of each scenario (Figure 3), it is clear the difference between the scenario *9 Images 10m* in relation to the others, presenting a spot of concentrated pixels with STR values from 4 to 14, and of NDVI between 0.2 and 0.8, making it difficult to identify the upper limit of the trapezoid. The large volume of data contained in the 10 meter pixel scenario presented greater parameterization difficulties, which was remedied by the resampling of the pixels to coarser resolutions (60 and 120 meters), however, it must be verified that a number of important information may have been lost in this transformation.

Through the use of masks of interest zones, pixels were located in several regions in the scatter plots (Figure 5). It is possible to observe the pixels present in the region marked by the red ellipse represent edges of cloud shadows, which appear white in the STR images (Figure 5A, B and C). With the resampling, the larger the pixel size, the lower the concentration of points in that region of the scatter plot. Therefore, cloud shadows have a significant effect on the difficulty of visualizing the trapezoid, even in a small number, since only images with less than 10% cloud cover were chosen, being of great importance the removal of their shadows or the use of images totally free of clouds.

However, the resampling of the images also affected pixels present inside agricultural areas, represented by the pink ellipsoid, this fact may show that important data may have been lost for the parameterization of the model in the resampling process (Figure 5E).
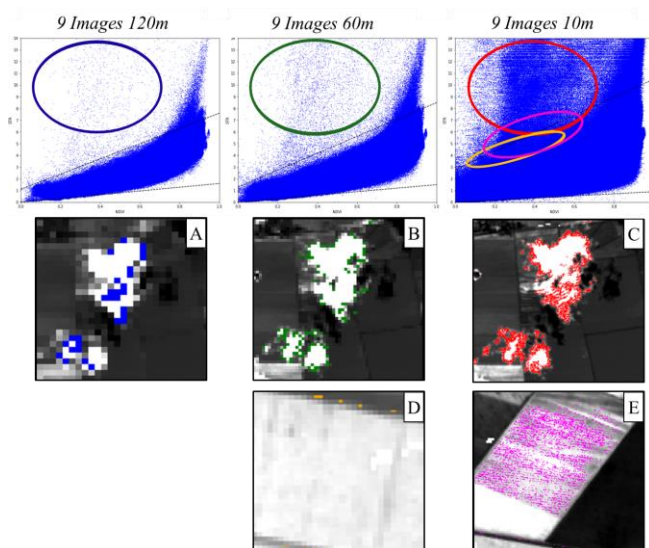
Figure 5. Location of pixels of different objects in the scatter plots created from 9 images with different resolutions. The boxes A, B, C, D and E indicates the pixels that are inside the blue, green, red, orange and purple ellipsoids, respectively.

There was also pixels present in borders of plots and roads. These pixels were concentrated in the region of the orange ellipse, which was smoothed in the resampling process (Figure 5D).

In the scatter plot of the scenario *9 Images without Mask and 120m*, there is a large concentration of pixels in the region of STR values greater than 8 and of NDVI greater than 0.8 (Figure 6).
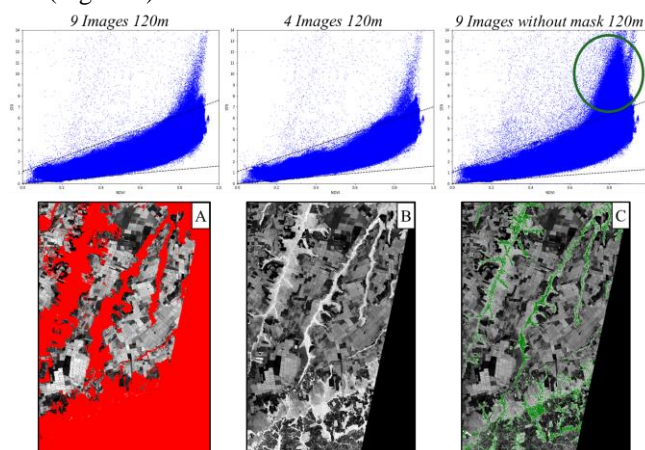

Figure 6. Location of pixels of different objects in the scatter plots created from different numbers of images and with removal of nonagricultural areas. In box A, the red area indicates the nonagricultural areas, the box B shows the NDVI of the scene extent, in box C the green points are the ones shown inside de green ellipsoid in the scatter plot.

The pixels concentrated in the region within the green ellipse are found near the drainage network present in the scene, which are covered by native vegetation (Figure 6C). This number of points did not influence the visual interpretation of the trapezoids, having equal results to that of the reference scenario (Table 3).

In the scenario of 4 Images and 120m, despite the similarities to the reference scenario, there was a fall in the area of the trapezoid, mainly in its upper limit, which may have caused differences in obtaining the coefficients, and consequently in the result of soil moisture.

Through the statistics, it is possible to observe that changes in the conditions of the parameterization of the model cause significant differences in results, especially in the case of pixel resampling. These differences may represent a variation of up to 40% in the soil moisture estimates (Table 2), especially in high humidity conditions.

5. CONCLUSIONS

The resampling of the pixels was the factor that caused the most differences in the soil moisture results, being related to large visual changes in the dispersion graphs.

There were no statistically significant differences between the scenarios of *9 Images without Mask and 120m* with the reference scenario.

It is necessary the conduction of validation studies with the purpose of clarifying which are the most favorable scenarios for the parameterization of OPTRAM.

AKNOWLEDGEMENTS

6. REFERENCES

[1] Sadeghi, M.; Babaeian, E.; Tuller, M.; Jones, S.B., The optical trapezoid model: A novel approach to remote sensing of soil moisture applied to Sentinel-2 and Landsat-8 observations. **Remote Sensing of Environment**, v. 198, p. 52–68, 2017.

[2] Peng, J.; Loew, A.; Merlin, O.; Verhoest, N.E.C., A review of spatial downscaling of satellite remotely sensed soil moisture. **Reviews of Geophysics**, v. 55, n. 2, p. 341–366, 2017.

[3] Sadeghi, M.; Jones, S.B.; Philpot, W.D., A linear physically-based model for remote sensing of soil moisture using short wave infrared bands. **Remote Sensing of Environment**, v. 164, p. 66–76, 2015.

[4]Louis, J.; Debaecker, V.; Pflug, B.; Main-Knorm, M.; Bieniarz, J.; Mueller-Wilm, U.; Cadau, E.; Gascon, F., Sentinel-2 Sen2cor: L2a processor for users. In: Living Planet Symposium, 2016, Prague, *Proceedings...* Prague: European Space Agency, 2016.

[5] Babaeian, E.; Sadeghi, M.; Franz, T.E.; Jones, S.; Tuller, M., Mapping soil moisture with the OPtical TRApezoid Model (OPTRAM) based on long-term MODIS observations. **Remote Sensing of Environment**, v. 211, n. April, p. 425–440, 2018.